11-1-2000

# Combined IR imaging-neural network method for the estimation of internal temperature in cooked chicken meat

Juan G. Ibarra
*University of Arkansas, Fayetteville*

Yang Tao
*University of Maryland, College Park*

Hongwei Xin
*Iowa State University*, hxin@iastate.edu

# Combined IR imaging-neural network method for the estimation of internal temperature in cooked chicken meat

**Abstract**

A noninvasive method for the estimation of internal temperature in chicken meat immediately following cooking is proposed. The external temperature from IR images was correlated with measured internal temperature through a multilayer neural network. To provide inputs for the network, time series experiments were conducted to obtain simultaneous observations of internal and external temperatures immediately after cooking during the cooling process. An IR camera working at the spectral band of 3.4 to 5.0 μm registered external temperature distributions without the interference of close-to-oven environment, while conventional thermocouples registered internal temperatures. For an internal temperature at a given time, simultaneous and lagged external temperature observations were used as the input of the neural network. Based on practical and statistical considerations, a criterion is established to reduce the nodes in the neural network input. The combined method was able to estimate internal temperature for times between 0 and 540 s within a standard error of ±1.01°C, and within an error of ±1.07°C for short times after cooking (3 min), with two thermograms at times t and t+30 s. The method has great potential for monitoring of doneness of chicken meat in conveyor belt type cooking and can be used as a platform for similar studies in other food products.

**Disciplines**

Agriculture | Bioresource and Agricultural Engineering

**Comments**

This article is from "Combined IR imaging-neural network method for the estimation of internal temperature in cooked chicken meat", *Opt. Eng.* 39(11), 3032-3038 (Nov 01, 2000). ; http://dx.doi.org/10.1117/1.1314595

# Combined IR imaging-neural network method for the estimation of internal temperature in cooked chicken meat

**Juan G. Ibarra,** MEMBER SPIE
University of Arkansas
Biological & Agricultural Engineering
    Department
203 Engineering Hall
Fayetteville, Arkansas 72701

**Yang Tao,** MEMBER SPIE
University of Maryland,
Biological Resources Engineering,
1426  Animal  Science/Agricultural
    Engineering Building,
College Park, Maryland 20742

**Hongwei Xin**
Iowa State University
Department of Agricultural and Biosystems
    Engineering
203 Davidson Hall
Ames, Iowa 50011-3080

**Abstract.** A noninvasive method for the estimation of internal temperature in chicken meat immediately following cooking is proposed. The external temperature from IR images was correlated with measured internal temperature through a multilayer neural network. To provide inputs for the network, time series experiments were conducted to obtain simultaneous observations of internal and external temperatures immediately after cooking during the cooling process. An IR camera working at the spectral band of 3.4 to 5.0 $\mu$m registered external temperature distributions without the interference of close-to-oven environment, while conventional thermocouples registered internal temperatures. For an internal temperature at a given time, simultaneous and lagged external temperature observations were used as the input of the neural network. Based on practical and statistical considerations, a criterion is established to reduce the nodes in the neural network input. The combined method was able to estimate internal temperature for times between 0 and 540 s within a standard error of $\pm 1.01°$C, and within an error of $\pm 1.07°$C for short times after cooking (3 min), with two thermograms at times $t$ and $t+30$ s. The method has great potential for monitoring of doneness of chicken meat in conveyor belt type cooking and can be used as a platform for similar studies in other food products. © *2000 Society of Photo-Optical Instrumentation Engineers.* [S0091-3286(00)00711-X]

Subject terms: thermal imaging; neural networks; chicken meat; food safety.

## 1  Introduction

As the demand for ready-to-eat meat products increases, the meat processors face a constant control problem in the cooking lines: To achieve the right cooking point in the meat products without over- or undercooking. To ensure microbial inactivation, the U.S. Department of Agriculture (USDA) requires[1] that every meat product in the line must reach a minimum internal temperature (71°C for chicken breast). Overcooking can ensure food safety; however, the products can have a diminished yield due to losses in water content, taste, and juiciness. To date, there is no real-time assay that can check the internal temperature of all meat products coming out the oven.

Because no contact with the surface is needed, infrared (IR) thermometry can be used for accurate and noninvasive inspection of cooking processes without detriment of food safety. The development of IR techniques in the cooking lines would aid quality control personnel in industrial cooking lines to comply with food safety regulations for ready-to-eat meat, while maintaining quality of the products. IR imaging techniques have been proposed for noncontact inspection in different applications.[2–4] In particular, active research is conducted for the applications of IR imaging techniques in agriculture. In an early work, Danno et al.[5] used an IR vidicon camera to evaluate the degree of maturity in certain fruits and tomato. The changes in the me-

tabolism of the vegetables generated heat that could be detected by the imaging device. More recently, Tao and Wen[6,7] used near- and mid-IR imaging to accurately detect defects in apples and to distinguish the defect from stem end/calyx (flowered end) with high accuracy.

To the best of our knowledge, the first attempt to use an IR camera in a cooking process was done by Goedeken et al.[8] In that work, an IR camera working in the spectral range 8 to 12 $\mu$m was used to monitor the surface temperature of food products cooked in a microwave oven. They required a compensation in emissivity for accurate surface temperature measurements. Recently, Ibarra et al.[9] used a IR focal planar array camera with working spectral range of 3.4 to 5.0 $\mu$m for the estimation of internal temperature in just-cooked chicken meat. The external temperature registered in the thermograms was correlated with the internal temperature through a linear time series model. Such a model was able to predict the internal temperature in the meat with three IR images at times 0, 60 and 150 s immediately after cooking. However, the use of linear models might reduce the accuracy of the estimation due to the nonlinear nature of heat transfer processes.

Here, the work initially developed in Ref. 9 was continued with the application of neural networks for the correlation between internal (IT) and external (ET) temperatures in chicken meat immediately after cooking. Time series

experiments were conducted to obtain simultaneous observations of IT and ET in just-cooked chicken meat, every 30 s for 570 s during the cooling process. A Levenberg-Marquardt neural network was used for the correlation between IT and ET. This hybrid algorithm provides speed and convergence to the network, which are sometimes a problem with conventional backpropagation algorithms. To estimate the optimum input for the network (and ultimately the number of IR images required for the IT estimation) some inferences were established based on the values of the correlation factors derived from the covariance matrix of IT values and simultaneous and lagged ET observations.

In Section 2, the experimental setup and the time series experiments are described. In Section 3, the neural network architecture and the optimization method are analyzed. In Section 4, the results of the network for times between 0 and 540 s are presented. Two cases are analyzed to verify the proposed heuristic criterion. In Section 5, the performance of the network for short times (up to 3 min) is presented. This analysis enabled evaluating the potential for a practical application. In Section 6, the conclusions of the work and some observations for a potential application are presented.

## 2 Experimental Setup

Time series experiments were conducted to provide data for the supervised neural network. In these experiments, simultaneous measurements of IT and ET were obtained starting immediately after the cooking process. The temperature measurements were taken every 30 s for 10 min during the cooling process. In this manner, sequential inputs (external temperature) and targets (internal temperature) were obtained for the supervised learning.

A total of 60 chicken breast samples with similar shape (average thickness after cooking of 11 mm) were cooked at the same oven temperature (177°C) for times between 5.8 and 7.6 min in a multipurpose industrial oven (model MPO-D2012 from Heat and Control, Inc.). The variation in cooking times allowed obtaining endpoint temperatures ranging from under- to overcooking.

A ThermaCAM PM250 (Inframetrics, Inc.) IR camera with spectral band of 3.4 to 5.0 $\mu$m (outside the water vapor sensitive band of 5 to 8 $\mu$m) was used to register external temperature distributions. The camera was located 1 m above the just-cooked samples and calibrated for background temperature compensation to minimize heat energy emission from the surroundings. In the recorded IR image, the external temperature of a fixed region of interest close to the thermocouple was measured, maintaining the size and location of the region of interest during all observations. Figure 1(a) shows an IR image of a batch of four chicken meat samples recorded in the conditions just described. The color table to the left of the thermogram represents the temperature codification. To register internal temperatures, embedded copper/constantan thermocouples (diameter 2.5 mm, response time 0.4 s) were inserted in the center of the thickest regions of the meat pieces. The IT readings were automatically recorded in a computer starting simultaneously with IR image recording. Room temperature was also registered with an additional thermocouple. A typical temperature versus time plot is shown in Fig. 1(b). Both internal and external temperature experi-
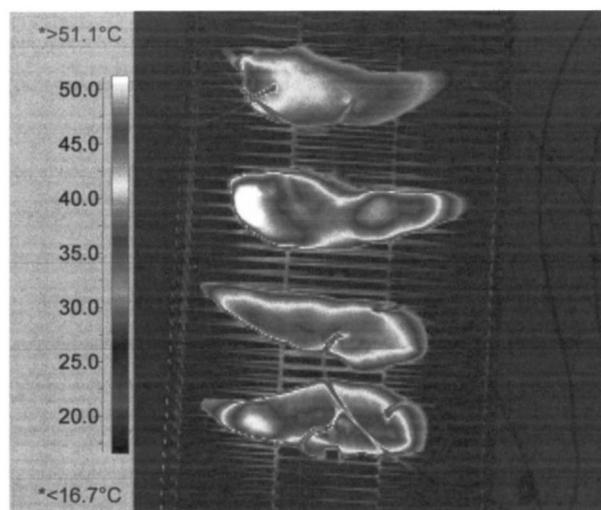


(a)
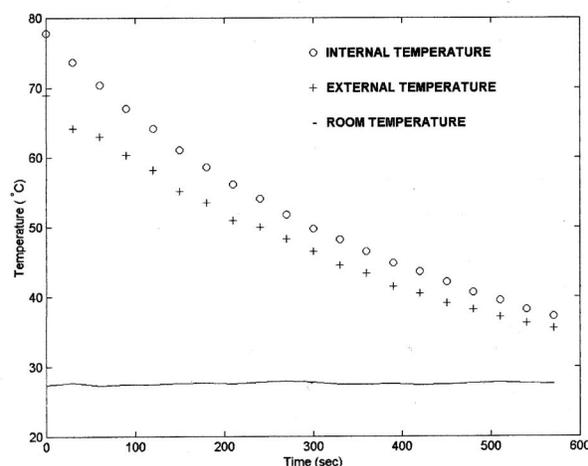


(b)

**Fig. 1** Thermograms and temperature time series: (a) IR image of a batch of four chicken fillets cooked simultaneously (note the table to the left indicates the false color codification of temperature distribution), and (b) typical exponential behavior of temperatures in time.

enced an exponential-decay behavior in time, which is typical in cooling processes.[10] Notice that there is a difference between initial internal and external temperatures and that both temperatures converged to the room temperature after a long time.

Four chicken breast samples were cooked at the same cooking time and imaged simultaneously. For each batch of four cooked samples, eight thermocouples were used (two for each sample). A total of 15 batches were cooked and imaged in this manner. Eight internal and eight external time series were obtained for each batch, each time series containing 20 time points equally spaced every 30 s. Because the cooking process changed the chemical and physical properties of the meat, experiments were conducted[11] to measure the emissivity of cooked chicken meat during and after cooking. It was observed that although the emissivity varies during the cooking process, it remains fairly constant after cooking. A constant emissivity of 0.63 was measured for chicken meat after cooking, and this value was used for all experiments.
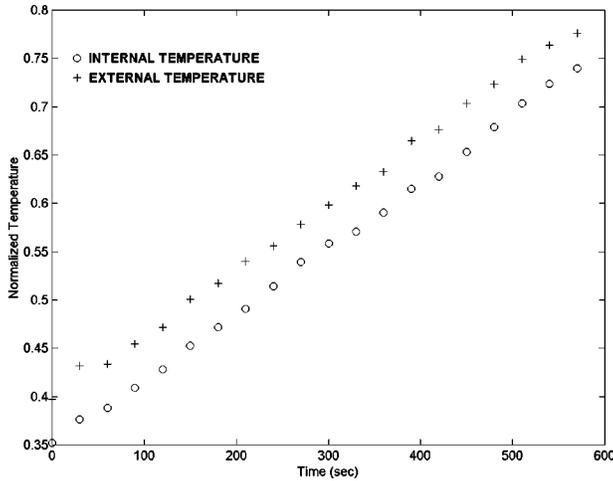
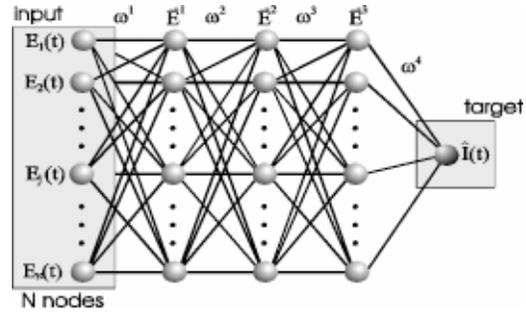**Fig. 2** Normalized temperature time series.



**Fig. 3** Five layer feedforward network architecture. The output $\hat{I}(t)$ is the estimated internal temperature at time $t$. The input $\mathbf{E}(t)$ is composed of simultaneous and lagged observations of external temperature. The matrix $\omega^i$ contains the weight factors between the layer $\mathbf{E}^i$ and the previous layer.

For convenience, the temperature observations were converted to the normalized quantities

$$I(t) = \frac{T_{\text{room}}(t)}{IT(t)},$$

$$E(t) = \frac{T_{\text{room}}(t)}{ET(t)}. \tag{1}$$

The unitless quantities in Eq. (1) are referred hereafter as normalized internal and external temperatures, respectively. The normalized temperatures defined in Eqs. (1) have the advantage of considering environment temperature variations, and to convert the input to numbers less than one, which are more suitable for the neural network algorithm. Figure 2 shows the typical normalized temperature behavior in time.

## 3 Neural Network Architecture

### 3.1 Levenberg-Marquardt Neural Network

A multilayer neural network was used to correlate an estimated normalized internal temperature at time $t$, $\hat{I}(t)$, in terms of the simultaneous normalized external temperature observation, $E(t)$, and some other lagged values, $E(t + n\Delta)$ still to be determined, where $1 \leq n \leq 19, \Delta = 30$ s. The input vector of normalized external temperatures is denoted as $\mathbf{E}(t)$, with components $E_i(t)$, $(i = 1, \ldots, N)$, where $N$ is the number of nodes in the input layer (to be specified later). A network with five hidden layers, which relates the normalized external temperature input, $\mathbf{E}(t)$, to $\hat{I}(t)$ is depicted in Fig. 3.

The nodes in the first hidden layer, $\mathbf{E}^1$ are calculated in terms of the input as

$$E_m^1 = \sigma\left(\sum_{j=1}^{N} w_{jm}^1 E_j(t) + b_m^1\right), \tag{2}$$

where $w_{jm}^1$ ($1 \leq j, m \leq N$) is the weight factor between input node $j$ and hidden layer node $m$, $b_m^1$ is a bias value initialized as 1, and $\sigma$ is the log-sigmoid function defined as

$$\sigma(x) = \frac{1}{1 + e^{-x}}. \tag{3}$$

The final layer, the targeted internal temperature $\hat{I}(t)$, is expressed in terms of the last hidden layer, for the case of five layer network as

$$\hat{I}(t) = \sigma\left(\sum_{j=1}^{N} w_j^4 E_j^3(t) + b\right), \tag{4}$$

with $b$ a final bias value. A detailed description of feedforward networks can be found in Ref. 12.

In the learning process, each time an input is presented to the network, the weight factors are adjusted to minimize a function of the error, $\varepsilon$, with a random guess for initial weight factors. The error is defined as the difference between the output of the network, $\hat{I}(t)$, and the actual observation or target, $I(t)$. Explicitly,

$$\varepsilon = I(t) - \hat{I}(t). \tag{5}$$

For the Levenberg-Marquardt algorithm, the function of the error to be minimized is the mean square error.

The most common way to minimize the mean square error is with the gradient descent method.[12] In this method, the weights are adjusted by moving along the negative gradient in small steps. This step factor is known as learning rate and denoted here as $\mu$. With a proper selection of the learning rate this method guarantees convergence, but it can take a very large number of iterations. A faster option is the Gauss-Newton method.[12] Table 1 compares the advantages and disadvantages of the methods mentioned. This method can lead rapidly to the minimum mean square error, but if the guess of initial weight factors is wildly incorrect, the algorithm can diverge. The situation is even worse because of the approximated calculation of required derivatives.

**Table 1** Characteristics of different algorithms for backpropagation neural networks.

| Algorithm | Speed | Convergence |
|---|:---:|:---:|
| Gradient Descent | | ● |
| Gauss-Newton | ● | |
| Levenberg-Marquardt | ● | ● |

The Levenberg-Marquardt algorithm provides a convenient compromise between the speed of Gauss-Newton method and the ensured convergence of gradient descent. In the first iteration, the algorithm begins with a gradient descent with a small learning rate $\mu_1$. If the mean square error is not small, then $\mu_2 = \mu_1 \theta$ is chosen in second iteration, where $\theta \gg \mu_1$. Eventually, the gradient descent algorithm should decrease the mean square error. If, after comparison with targeted internal temperature, the mean square error for $k$'th iteration is small enough, then $\mu_{k+1} = \mu_k / \theta$ is chosen, and the algorithm will be approaching the Gauss-Newton method. The details of Levenberg-Marquardt algorithm can be found in Ref. 13. Sometimes during calculation a small mean square error is reached quickly, and no significant reduction is achieved with further calculation. Then, it is convenient to define an error goal, $\langle \varepsilon_g^2 \rangle$, for early stopping. This is also useful when the algorithm is not converging. In practice, the learning rate $\mu$ and the error goal $\langle \varepsilon_g^2 \rangle$ are specified by trail and error.

Once the network is designed, the normalized external temperature vectors must be selected to produce an optimum output, with the fewest number of elements. This is discussed next.

## 3.2 Network Input Reduction and Optimization

The neural network design will be complete with the specification of the input vector $\mathbf{E}(t)$; that is, to establish the number of nodes and lags included in the input. Initially, the input can have 20 nodes, which is the number of time points in each series. Because each input node represents an IR image, the use of all the 20 external temperature observations in a particular time series to estimate a given internal temperature, will require 570 s (with 30 s lag between each IR image). Considering that in an actual industrial cooking process the meat products are traveling typically at a speed of 0.2 to 0.3 m/s, a distance greater than 110 m will be required to register the last IR image (at 570 s). As a consequence, a reduction in the number of input nodes is needed to increase the potential application of this work.

A first reduction in the number of input nodes can be achieved by assuming that only six lags significantly contribute to the estimation. Specifically, for an internal temperature target at time $t$, $I(t)$, only the simultaneous external temperature value $E(t)$ and up to five lagged values, $E(t+n\Delta)$ $(1 \leq n \leq 5)$, are assumed to contribute significantly to the internal temperature. In this case, the maximum time required for the internal temperature estimation is 2 min, which will require a minimum traveling distance in the conveyor belt of 36 m.

Further reduction in the number of input nodes can be achieved by considering the contribution of the possible

input nodes to the internal temperature. It is reasonable to think that the internal temperature time series is strongly correlated to the simultaneous external temperature time series, and that the correlation decreases for lagged values. A way to measure that correlation is to consider the covariance between the normalized IT and the ET time series without lag, with one lag and so on. Explicitly, if for a pair of normalized internal and external temperature time series, the set of variables for the covariance analysis is arranged in the matrix

$$\mathbf{X} = \begin{bmatrix} I(t) & E(t) & - & \cdots & - \\ I(t+\Delta) & E(t+\Delta) & E(t) & \cdots & - \\ \vdots & \vdots & \vdots & & \vdots \\ I(t+5\Delta) & E(t+5\Delta) & E(t+4\Delta) & \cdots & E(t) \end{bmatrix},$$

(6)

then the elements in the covariance[14] matrix are expressed as

$$s_{ik} = \frac{1}{6} \sum_{j=1}^{6} x_{ij} x_{kj} - \frac{1}{30} \sum_{j=1}^{6} x_{ij} \sum_{j=1}^{6} x_{kj},$$

(7)

with $i = 1, \ldots, 4$ and $1 \leq k \leq 6$. The corresponding correlation coefficients are defined[14] as

$$r_{ik} = \frac{s_{ik}}{s_i s_k},$$

(8)

with $s_i^2 \equiv s_{ii}$. The covariance matrix of the data indicates if there exists a linear relationship between the time series in matrix $\mathbf{X}$, and the associated correlation factors indicate the strength of that relationship. Furthermore, because there is interest only in the relationship between the internal temperature and the lagged external temperatures, only the cases $i = 1$, $2 \leq k \leq 6$ are considered. Therefore, a high correlation coefficient $r_{12}$ indicates a strong relationship between simultaneous internal and external temperatures and so on. In this manner, the input vector $\mathbf{E}(t)$ can be reduced by including only the nodes with higher correlation coefficient. Although this heuristic criterion is not directly related to the neural network algorithm, it can be useful for the simplification of network input. Similar reductions, as principal components analysis, are often used for this purpose.[12]

The covariance matrix elements in Eq. (7) and the corresponding correlation factors in Eq. (8) were calculated from the time series data of all batches. The components in matrix $\mathbf{X}$ [see Eq. (6)] were obtained by averaging the normalized internal and external time series. The results of this computation are presented in Fig. 4. The vertical axis in the figure corresponds to the square value of the correlation coefficient, $r_{1m}^2$ ($2 \leq m \leq 7$), and the horizontal axis corresponds to the lag index $m$. As expected, the correlation is high for the simultaneous ($m=2$) internal and external temperature time series, and gradually decreases for the lagged external temperature time series. It can be observed in Fig. 4 that $r_{12}^2 = 0.999$ and $r_{13}^2 = 0.906$ are the highest correlation factors. This indicates that an input with simul-
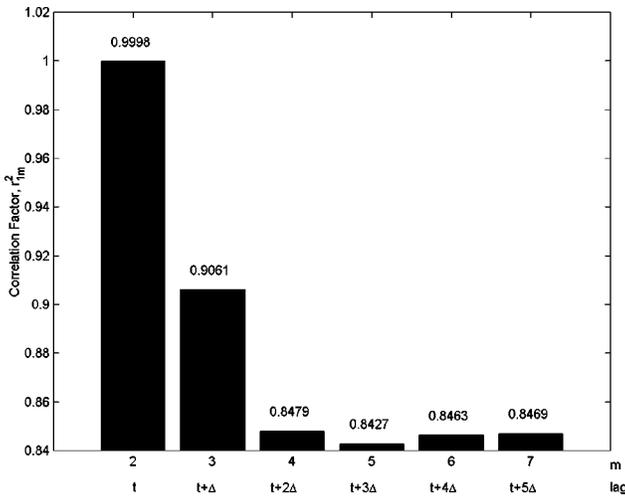
**Fig. 4** Results of covariance matrix criterion. The vertical axis corresponds to the square of the correlation coefficients of the covariance matrix $r_{1m}^2$. The horizontal axis corresponds to the lag in terms of $\Delta$.



**Fig. 5** Performance parameter for case [01]. The parameter $P$ measures the agreement between actual and estimated internal temperatures. Results show that a five-layer network has better performance.

taneous and one-lag external temperature may be enough for internal temperature estimation. This situation is labeled hereafter as case [01]. The notation indicates the number of nodes and order of lags in the input. The case [012] is for an input with simultaneous, one-lag, and two-lag external temperature values (see next section).

In a practical application, the reduction of the input to two components means that for the estimation of the internal temperature at certain time (say immediately after cooking) it is needed to take an IR image at that time, and a second IR image after 30 s. This fact increases the potential for a practical implementation.

## 4 Performance of the Network During Cooling Time

A total of 120 time series separated in 15 batches were obtained in the experiments. The data were separated into training and test sets in such a manner that data from all batches and all thermocouples were evenly distributed among the training and test sets. A total of 60 time series were used in the training set and the remaining 60 series in the test set.

To verify the heuristic criteria given in the last section, the performances of the network for cases [01] and [012] are presented next.

### 4.1 Case [01]

In this case $N=2$, and for an internal temperature target $I(t)$ the corresponding external temperature input is expressed as

$$\mathbf{E}(t) = \begin{bmatrix} E(t) \\ E(t+\Delta) \end{bmatrix}. \tag{9}$$

Training data were presented to the multi-layer Levenberg-Marquardt network with fixed learning rate $\mu = 1.0$ and performance goal $\langle \varepsilon_g^2 \rangle = 3.1 \times 10^4$. A total of 1040 inputs were used for the training. The optimal number
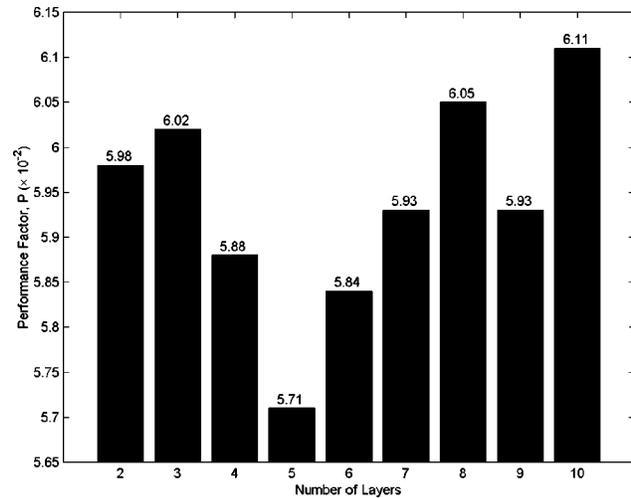
of layers for internal temperature estimation was found by presenting the training data to the network with two up to ten layers. Then the obtained network was simulated with the testing data (1040 inputs) and the performance of each multilayer network was evaluated and compared. The comparison was done through a regression analysis between the pairs of actual and estimated internal temperatures, $(I(t), \hat{I}(t))$ in the test data set. Therefore, the performance of the network can be evaluated from the regression parameters. A good performance corresponds to a slope, $S$, close to one, an intersection $I_0$, close to zero, and a high $R^2$. The standard error and the residuals are also good indicators. A simple way to measure the network performance with the proposed regression analysis is by defining the performance parameter

$$P = (1 - R^2) + |1 - S| + |I_0|. \tag{10}$$

A perfect match corresponds to $P = 0$ and the agreement decreases as $P$ increases. Note that for good agreements $P \sim |I_0|$, so the value of the performance parameter depends on the range of the normalized internal temperature. This parameter is useful only when comparing different performances of the same quantities, as is the case here. The results of these calculations are shown in Fig. 5. The results indicate that the optimal performance is for a five-layer network. Overfitting is a frequent problem with neural networks. Sometimes using more layers than required produces a good matching with the training set, but the agreement with the test set is poor. Unfortunately, there is no method to specify the optimal number of layers but testing different cases. Usually, a good agreement can be found with five or fewer layers.

With this architecture a very good performance was obtained with a slope of 0.983, an intercept at 0.92°C, and $R^2 = 0.988$ The standard error of the estimation was $\pm 1.01$°C with standard residuals between $-4$ and 4°C. The network finished the estimation after 92 iterations.

### 4.2 Case [012]

The analysis described in last subsection was repeated for the input

$$\mathbf{E}(t) = \begin{bmatrix} E(t) \\ E(t+\Delta) \\ E(2+2\Delta) \end{bmatrix}, \qquad (11)$$

extracted from the training set. The input in Eq. (11) indicates that for temperature estimation, three IR images are needed at times $t$, $t+30$ s, and $t+60$ s. As in the previous case, a five layer network was optimal for the estimation. The algorithm used $\mu = 1.0$, with a performance goal of $1.1 \times 10^4$. The network was trained for 772 epochs before it reached the goal. The obtained network was simulated with the test set and again, a regression analysis was used to evaluate the performance of the network. The parameters found in this case were $S = 0.980$, $I_0 = 1.10°C$, and $R^2 = 0.986$. The standard error of the estimation was $\pm 1.05°C$ with similar standard residuals as for the case [01]. Although the regression parameters indicate a good performance of the network, the parameters obtained in the case [01] indicate a slightly better performance. The performance decreased for other cases. For instance, for [0123] (not illustrated here), a slope $= 0.980$, intercept at $1.70°C$, and $R^2 = 0.977$ were found. Moreover, the residuals and standard error were bigger than in the two previous cases.

An additional advantage of the use of a small number of inputs is the reduction of the IR images required. According to the findings presented here, only two thermograms and 30 s are needed for a good estimation.

### 5 Performance of the Network Immediately After Cooking

Although the proposed neural network can estimate the internal temperature during the cooling process, more interesting is the estimation for times shortly after cooking. A total of 120 inputs can be extracted from the 15 time series for time $t = 0$ (immediately after cooking). Unfortunately this number of inputs was not enough for a proper training and testing of the network. To increase the number of inputs, the first five temperatures in each time series were taken. In this manner, 260 inputs were used for training and 260 for test. Because of the short number of lags available, only $k = 2$ was considered in this case. As in the cases described in the last section, an architecture of five layers was used, considering a learning rate of 1 with a performance goal of $1.2 \times 10^{-4}$. The goal was reached after 297 epochs and the network was simulated with inputs from the test set. A slope $= 0.966$, intercept at $1.89°C$, and $R^2 = 0.974$ were found. Although the performance of the network has decreased in this case, the standard error obtained was $\pm 1.03°C$ and residuals were basically between $-2°C$ and $2°C$.

To improve the performance for endpoint temperatures, a higher number of inputs must be provided. In addition, it must be considered that in the transit from the oven cavity to the environment occurred transient heat transfer effects that must be included.

The internal temperature estimation immediately after cooking allow evaluating the endpoint temperature of the meat.

### 6 Conclusions

A noninvasive method for the estimation of internal temperature of just-cooked meat was developed. The method combines thermovision for external temperature recording of chicken breast fillets immediately after cooking with a Levenberg-Marquardt backpropagation algorithm for the correlation with internal temperature observations. Simultaneous internal and external temperature time series were obtained for observations every 30 s for 10 min during the cooling process immediately after cooking. The input vectors of the network were composed of simultaneous and lagged observations of external temperature to target the corresponding internal temperature at a given time.

To optimize the input vectors, a heuristic method based on the covariance matrix of the internal temperature time series and simultaneous and lagged external time series was proposed. It was found that the optimum input was formed by external temperature observations at time $t$ and $t + 30$ s. The method was verified for two cases.

The network was trained and then simulated with test data. The performance of the network was very good and internal temperature was estimated within a standard error of $\pm 1.01°C$ for times between 0 and 540 s after cooking, for under-, over- and right-cooked chicken meat samples. For initial times (up to 3 min), the network estimated internal temperature within an error of $\pm 1.03°C$ with two IR images at $t$ and $t + 30$ s lags. The combined thermovision-neural network method can be used as a calibration procedure for non-invasive endpoint temperatures in just cooked chicken meat.

Future research is needed for a real-time application. First, the samples used in the experimentation had similar shape and thickness. This is not the usual case. Samples as whole chicken breast present a very irregular shape that can certainly affect the relation between internal and external temperature. As a consequence, it is needed to include the thickness variation of the sample in the network input. Research is planned to extract the 3-D shape of a chicken breast with a range technique, and to combine this information with the thermogram. Another important factor is the transient effect that may be present in the transit from the oven. A cooling chamber can aid to stabilize the temperature observations for times immediately after cooking. Also, to improve the performance of the network for endpoint temperatures, time series must be obtained for shorter times and with reduced lags. The IR camera employed showed to be suitable for the proposed method. The fact that only two IR images were required for internal temperature estimation enables using only one IR camera with suitably located IR mirrors to register at the required lags. Note that although the proposed method requires 30 s for the internal temperature estimation, the method can achieve real-time estimation in a streamline situation. That is, it is not neccesary to wait for that period to start the estimation in the next chicken product but, with proper synchronization, the IR camera can continuously register the thermograms and the estimation can be done as the products are traveling in a conveyor belt.

IR imaging techniques have the potential for high-speed and noninvasive inspection of cooked food products. The method proposed here can be used as a platform for similar studies in other types of food products, and after further improvement, can be used as a real-time assay for the verification of endpoint temperatures in industrial cooking lines.

## References

1. USDA-FSIS, ''Requirements for the production of poultry breakfast strips, poultry rolls, and certain other poultry products,'' Animals and Animal Products, Part 381.150, pp. 491–192 of Chapter 3 in Title 9 of the *Code of Federal Regulations*, Office of the Federal Register, National Archives and Records, Washington, DCUSDA-FSIS (1992).
2. P. J. Kirby, ''Measuring hot metals on the move,'' *ICS* **65**, 25–28 (1992).
3. M. Zong, J. Zhang, and Y. Zhao, ''Pulse-heating infrared thermography non-destructive testing technique,'' *Proc. SPIE* **2899**, 654–659 (1996).
4. J.-F. Pelletier and X. Maldague, ''Shape from heating: a two-dimensional approach for shape extraction in infrared images,'' *Opt. Eng.* **36**, 370–375 (1997).
5. A. Danno, M. Miyazato, and E. Ishiguro, ''Quality evaluation of agricultural products by infrared imaging method. III. Maturity evaluation of fruits and vegetables,'' *Mem. Fac. Agr. Kagoshima Univ.* **16**, 157–164 (1980).
6. Y. Tao and Z. Wen, ''Item defect detection apparatus and method,'' U.S. Patent File No. 09/046,270, pending, Attny. Ref. ARK-00798198 (1988).
7. Y. Tao and Z. Wen, ''Apple defect detection (fruit defect and stem/calyx recognition system),'' U.S. Patent File No. 09/046,454, pending, Attny. Ref. ARK-00798198 (1998).
8. D. L. Goedeken, C. H. Tong, and R. R. Lentz, ''Design and calibration of a continuous temperature measurement system in a microwave cavity by infrared imaging,'' *J. Food Proc. Preserv.* **15**, 331–337 (1991).
9. J. G. Ibarra, Y. Tao, J. Walker, and C. Griffis, ''Internal temperature of cooked chicken meat through infrared imaging and time series analysis,'' *Trans. ASAE* **42**, 1383–1390 (1999).
10. I. Dincer and O. F. Geniceli, ''Cooling process and heat transfer parameters of cylindrical products cooled both in water and in air,'' *Int. J. Heat Mass Transf.* **37**, 625–633 (1994).
11. J. G. Ibarra, Y. Tao, A. Cardarelli, and J. Shultz, ''Cooked and raw chicken meat: emissivity in the mid-infrared region,'' *Appl. Eng. Agr.* **7**, 129–131 (2000).
12. M. T. Hagan, H. B. Demuth, and M. Beale, *Neural Network Design*, Chap. 9, PWS Publishing Company, Boston (1996).
13. L. E. Scales, *Introduction to Non-Linear Optimization*, Chaps. 8, 9, and 12, Springer-Verlag, New York (1985).
14. J. E. Jackson, *A User's Guide to Principal Components*, Wiley, New York (1991).

**Juan G. Ibarra** is a physicist with majors in solid state physics and optics. His graduate studies were at the University of Puebla and the National Institute of Astrophysics, Optics and Electronics (both in México) for his MS and PhD, respectively. Currently, he is a research associate in the Bio & Ag Engineering Department at the University of Arkansas. His research includes machine vision for food inspection, infrared thermography, and optical systems for agricultural applications. He was recently honored with the 2000 Superior Paper Award from the American Society of Agricultural Engineers (ASAE). He is a member of the ASAE and SPIE.

**Yang Tao** received his BS from Nanjing Institute of Technology, China, in 1982, his MS from the University of Nebraska, Lincoln in 1988, and his PhD in 1991 from the Pennsylvania State University. He was the vice-president of research and development at Agri-Tech, Inc. Currently, he is an associate professor of biological resources engineering at the University of Maryland. During his career, he has been the research leader and principal investigator of several projects related to machine vision intelligence of on-line inspection, including the ASAE award winning MERLIN® high-speed color vision sorter, for outstanding innovation in technology. He was awarded the 1994 Engineering Achievement of the Year Young Designer Award from the ASAE. Dr. Tao is a member of ASAE and SPIE.

**Hongwei Xin** is an associate professor of the Department of Agricultural and Biosystems Engineering, Iowa State University, Ames, Iowa. His academic interests and activities include quantification of effects of biophysical factors on animal production and well-being, application of bio-imaging to enhance animal well-being and production efficiency, and improvement of air quality in animal production facilities. He is the author or co-author of 45 refereed journal articles, four of which received the ''Superior Paper'' or ''Honorary Mention Paper'' Awards from the American Society of Agricultural Engineers (ASAE).